A Mössbauer study of the oxidation state of Fe in silicate melts

Kasthuri D. Jayasuriya,[1,*] Hugh St.C. O'Neill,[2,†] Andrew J. Berry,[2] and Stewart J. Campbell[1]

[1]School of Physical, Environmental and Mathematical Sciences, University of New South Wales, Australian Defence Force Academy, Canberra, ACT 2600, Australia
[2]Research School of Earth Sciences, Australian National University, Canberra, ACT 0200, Australia

Abstract

$Fe^{3+}/\Sigma Fe$ ratios were determined from Mössbauer spectra recorded for a series of 17 anorthite-diopside eutectic glasses containing 1 wt% $^{57}Fe_2O_3$ quenched from melts equilibrated over a range of oxygen fugacities from $f_{O_2} \sim 10^5$ bars ($Fe^{3+}/\Sigma Fe = 1$) to 10^{-13} bars ($Fe^{3+}/\Sigma Fe = 0$) at 1682 K. Fe^{3+}/Fe^{2+} was found to be proportional to f_{O_2} to the power of 0.245 ± 0.004, in excellent agreement with the theoretical value of 0.25 expected from the stoichiometry of the reaction $Fe^{2+}O + 0.25\,O_2 = Fe^{3+}O_{1.5}$. The uncertainty in the $Fe^{3+}/\Sigma Fe$ ratios determined by Mössbauer spectroscopy was estimated as $\pm$ 0.01 (1σ) from the fit of the data to the theoretical expression, which is significantly less than that quoted for previous measurements on silicate glasses; this results from fitting the spectra of a large number of systematically varying samples, which allows many of the ambiguities associated with the fitting procedure to be minimized. $Fe^{3+}/\Sigma Fe$ ratios were then determined for samples of the anorthite-diopside eutectic composition equilibrated at selected values of f_{O_2}, to which up to 30 wt% Fe_2O_3 had been added. $Fe^{3+}/\Sigma Fe$ was found to vary with ΣFe (or FeO_T), but both the 1 wt% and high FeO_T data could be satisfactorily fit assuming the ideal stoichiometry (i.e., $Fe^{3+}/Fe^{2+} \propto f_{O_2}^{1/4}$) by the inclusion of a Margules term describing Fe^{2+}-Fe^{3+} interactions. The large negative value of this term indicates a tendency toward the formation of Fe^{2+}-Fe^{3+} complexes in the melt. The resulting expression, using the ideal exponent of 0.25, gave a fit to 289 $Fe^{3+}/\Sigma Fe$ values, compiled from various literature sources, of similar quality as previous empirical models which found an exponent of ~0.20. Although the empirical models reproduce $Fe^{3+}/\Sigma Fe$ values of glasses with high FeO_T reasonably well, they describe the data for 1 wt% FeO_T poorly. The non-ideal values of the exponent describing the dependence of $Fe^{3+}/\Sigma Fe$ on f_{O_2} at high FeO_T are an artifact of models that did not include a term explicitly to describe the Fe^{2+}-Fe^{3+} interactions. An alternative model in which Fe in the silicate melt is described in terms of three species, $Fe^{2+}O$, $Fe^{3+}O_{1.5}$, and the non-integral valence species $Fe^{2.6+}O_{1.3}$, was also tested with promising results. However, at present there is no model that fits the data within the assessed accuracy of the experimental measurements.

Introduction

In most terrestrial magmas, Fe is overwhelmingly the most abundant element occurring in more than one oxidation state, namely as Fe^{2+} and Fe^{3+}. The ratio of these oxidation states (conveniently described as $Fe^{3+}/\Sigma Fe$) varies widely in different magma types (Carmichael 1991), and is well known to influence many of the physical and chemical properties of the magma, such as melt structure and viscosity. The $Fe^{3+}/\Sigma Fe$ ratio is one factor determining the temperature and composition of crystallizing phases. Due to the high abundance of Fe relative to other redox-variable elements, the $Fe^{3+}/\Sigma Fe$ ratio should control the oxygen fugacity (f_{O_2}) of a magma, and therefore the valencies of heterovalent trace elements and the speciation of volatile components.

The $Fe^{3+}/\Sigma Fe$ ratio is related to the oxygen fugacity by the reaction:

$$Fe^{2+}O + 1/4\,O_2 = Fe^{3+}O_{1.5} \quad (1)$$
$$\text{silicate melt} \qquad \text{silicate melt}$$
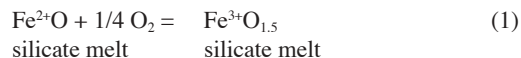
The stoichiometry of this relationship predicts that $Fe^{3+}/\Sigma Fe$ is proportional to f_{O_2} to the power of 0.25 (Kennedy 1948); this relationship was verified experimentally by Johnston (1964) for dilute concentrations of FeO_T, (where $FeO_T = Fe^{2+}O + Fe_2^{3+}O_3$), (~2 wt%) in $Na_2O \cdot 2SiO_2$ melts. However, subsequent experimental studies on geologically relevant melt compositions have repeatedly returned significantly lower values of this exponent. Fudali (1965) found exponents that ranged from 0.16 to 0.27 for the different melt compositions that he studied, with a tendency to cluster around 0.20. Sack et al. (1980) and subsequently Kilinc et al. (1983) both reported an exponent of 0.22 from a global fit to a simplified thermodynamic formulation of Equation 1. Their input data covered a large range of compositions appropriate to natural magmas, including both their own experimental data and previous work. Subsequent refitting by Kress and Carmichael (1991) with still more data lowered the apparent exponent to 0.20. Borisov and Shapkin (1990) refitted essentially the same data as

---

* Present address: Department of Physics, University of Kelaniya, Kelaniya, Sri Lanka.
† E-mail: hugh.oneill@anu.edu.au

Kilinc et al. (1983) to a formulation of the same type as suggested by Sack et al. (1980) but with an increased number of terms; this only made things worse, as the exponent decreased to 0.18.

The causes of this discrepancy remain controversial. An obvious possibility is that the formulation introduced by Sack et al. (1980) goes too far in its simplification of the thermodynamics to return a physically meaningful exponent. In particular, in melts with high FeO_T, if the activity coefficients of either FeO or $FeO_{1.5}$ vary either with their own concentration or with the concentration of the other (i.e., Fe^{2+}-Fe^{3+} interactions), there will be a systematic effect on the $Fe^{3+}/\Sigma Fe$ ratio that, because of the lack of suitable terms in the Sack et al. (1980) equation, would manifest itself in a deviation from the ideal value of the exponent. Kress and Carmichael (1988) later rationalized the use of a non-ideal exponent [which was 0.232 in their fit to the Sack et al. (1980) equation] by introducing the hypothetical species $FeO_{1.464}$ as one of the components in place of $FeO_{1.5}$, retaining FeO as the other component. This enabled them to rewrite the reaction as $FeO + 0.232 O_2 = FeO_{1.464}$, thereby achieving mass balance. Kress and Carmichael (1988) stated that the $FeO_{1.464}$ component corresponds to the formation of a complex with stoichiometry approximately $FeO \cdot 6Fe_2O_3$, but the thermodynamic logic of their approach implies that the Fe in this component is in a non-integral valence state, i.e., $Fe^{2.928+}$. Subsequently Kress and Carmichael (1989 and 1991, their Appendix) extended this approach by using three Fe-oxide components, FeO, $FeO_{1.5}$, and FeO_{1+y}, with y found empirically to be 0.3 by fitting data in the CaO-SiO_2-Fe-O system.

Here, we reinvestigate the problem of Fe redox equilibria in silicate melts by a detailed systematic study of the effects of both f_{O_2} and FeO_T concentration, keeping all other variables constant. We chose the Fe-free, anorthite-diopside eutectic composition as our starting point, and a temperature of 1682 K. We first studied this composition doped with ~1 wt% Fe_2O_3 and equilibrated over a log f_{O_2} range from –13 (fully reduced) to +4.8 (fully oxidized). This establishes the nature of the equilibrium in the low concentration region where Fe^{2+}-Fe^{3+} interactions may be expected to be minimal. We then examined the effect of adding FeO_T at three selected values of f_{O_2} (log f_{O_2} = 0, –4, and –7). $Fe^{3+}/\Sigma Fe$ was determined by Mössbauer spectroscopy of glasses (i.e., the quenched melts) at room temperature (RT), with a few additional analyses at liquid He temperature (4.2 K) to check suggestions that Mössbauer determinations of $Fe^{3+}/\Sigma Fe$ in silicate glasses at RT may be systematically in error due to a difference in the recoil-free fraction between Fe^{2+} and Fe^{3+}. The analysis of a large number of closely related samples enables the precision of the method to be evaluated.

Experimental methods

A composition corresponding to the anorthite-diopside eutectic (=AD_{eu}, nominally 42 wt% $CaAl_2Si_2O_8$ + 58 wt% $CaMgSi_2O_6$) was prepared from reagent grade MgO, Al_2O_3, SiO_2, and $CaCO_3$. For low Fe concentration samples, 1 wt% Fe_2O_3 containing 93.5 at% ^{57}Fe was added. Samples were also prepared at higher Fe concentrations with 2, 4, 7, 10, 20, or 30 wt% Fe_2O_3 being added to the AD_{eu} composition. In these experiments, mixtures of isotopically enriched and isotopically natural Fe_2O_3 were used to maintain a constant amount of ^{57}Fe in the sample. Samples were equilibrated at 1682 K in a vertical tube furnace (internal diameter 42 mm) equipped for gas mixing, with values of log f_{O_2} imposed between ~ 0 and –13, using the following gas mixtures (in order of decreasing f_{O_2}): O_2, air, CO_2-O_2, CO_2, CO_2-CO, and CO_2-H_2. Oxygen fugacity is given here in bars, relative to the

conventional standard state of O_2 at 1 bar and the temperature of interest. Details of gas flow rates are given in Table 1, together with the uncertainty in log f_{O_2} for each experiment. These were calculated assuming uncertainties of 0.5% in gas flow rates, ± 2 °C in temperature, and 0.02 bar in total pressure. Oxygen fugacity was checked in several runs using a $SIRO_2$ oxygen sensor (accuracy ± 0.02 in log f_{O_2}). There was complete agreement between the f_{O_2} calculated from the gas-mixing ratio and that determined by the sensor, within the combined uncertainties, except for run FeV10 where the discrepancy was 0.07 in log f_{O_2}.

Samples were mounted in the furnace on wire loops: Re for log f_{O_2} < –7, Ir for log f_{O_2} = –6, and Pt for log f_{O_2} ≥ –5. Rhenium strips (manufactured as filaments for mass spectrometry) provide an answer to the age-old experimental problem of Fe loss to Pt under reducing conditions (Borisov and Jones 1999; O'Neill and Mavrogenes 2002); but Re was reported by Borisov and Jones (1999) to volatilize by oxidation at log f_{O_2} > –8 at 1400 °C, which is exactly what we observed: the Re was volatilized completely in a few hours where it was not protected by the molten sample, and the loop failed. In order to obtain samples at log f_{O_2} = –7, we therefore wrapped Pt wire around the Re wire where it is exposed above the loop and hung the sample from the Pt. Iron loss into Pt was found to be excessive at log f_{O_2} = –6 and Ir wire was used for this condition. We eschewed the use of Fe-doped Pt alloys due to the risk of contaminating the ^{57}Fe samples from an extraneous source of isotopically normal Fe.

Most samples were equilibrated for >30 h (Table 1), which is longer than the time required to achieve equilibrium as found by previous similar studies (Thornber et al. 1980; Kilinc et al. 1983). Samples were then quenched rapidly by dropping into water, producing homogeneous glasses. An additional sample was prepared at P_{O_2} = 11 kbar and 1673 K by equilibration in a sealed Pt capsule containing 20 wt% PtO_2, using a piston-cylinder apparatus. Under these conditions, PtO_2 breaks down to Pt and sufficient O_2 to produce a partial pressure equal to the confining pressure. The value of log f_{O_2} at this pressure and temperature is calculated to be +4.8 from the equation of state of pure O_2 of Belonoshko and Saxena (1991).

The FeO_T content of all experiments with FeO_T > 1 wt% was checked by electron microprobe analysis using the EDS mode. Renormalizing these analyses to an FeO-free basis gave, in wt%, SiO_2 = 50.47(19), Al_2O_3 = 15.12(10), MgO = 10.46(12), and CaO = 23.94(16). The values in parentheses are observed standard deviations from 95 analyses on 16 samples. Neither magnetite, nor any other crystalline phase, was observed by back-scattered electron imaging in any of the samples.

Mössbauer spectra were obtained at room temperature (RT) and 4.2 K using a

TABLE 1. Sample preparation

Sample	log f_{O_2}	Gas mix (SCCM)		Time (h)	Wire loop
		FeO_T ~ 1 wt%			
		CO_2	H_2		
FeV19	–12.9 (2)	20.0 × 10	50.0 × 200	8	Re
		CO_2	CO		
FeV2	–10.90 (2)	60.0 × 10	47.0 × 200	45	Re
FeV20	–9.91 (3)	6.7 × 200	33.4 × 200	69	Re
FeV21	–8.90 (2)	20.0 × 200	31.0 × 200	21	Re
FeV5	–7.88 (2)	27.0 × 200	13.0 × 200	34	Re
FeV22	–6.91 (3)	40.0 × 200	6.3 × 200	22	Re/Pt
FeV12	–5.91 (2)	40.0 × 200	40.0 × 10	43	Ir
FeV6	–4.91 (2)	51.0 × 200	16.0 × 10	34	Pt
FeV15	–3.91 (4)*	51.0 × 200	5.1 × 10	38	Pt
FeV8	–3.01 (5)*	100.0 × 200	–	47	Pt
		CO_2	O_2		
FeV10	–2.42 (2)*	150.0 × 200	10.0 × 10	42	Pt
FeV11	–1.98 (1)*	98.0 × 200	20.0 × 10	44	Pt
FeV13	–1.50 (1)*	95.0 × 200	62.0 × 10	43	Pt
FeV14	–1.01 (1)*	45.0 × 200	100.0 × 10	48	Pt
FeV1	–0.69 (1)	air		38	Pt
FeV9	–0.01 (1)	–	100.0 × 200	39	Pt
D60	+4.8 (?)	O_2 at 11 kbar		4	sealed Pt capsule
		FeO_T ~ 2, 4, 7, 10, 20 and 30 wt%			
		CO_2	CO		
C27/11/01	–6.91 (3)	40.0 × 200	6.3×200	22	Re/Pt
C14/12/01	–3.91 (4)	51.0 × 200	5.1×10	57	Pt
			O_2		
D31/7/01	–0.01 (1)		100.0×200	22	Pt

Notes: All samples were equilibrated at 1409 °C, except the high pressure run (1400 °C nominal). Gas mix flow rates are given in standard cubic centimeters per minute (SCCM). The uncertainties in log f_{O_2} are calculated assuming uncertainties of 0.5% in gas flow rates, in temperature of ± 2 °C, and in total pressure of 0.02 bar.
* The f_{O_2} was checked directly using a $SIRO_2$ oxygen sensor.

constant acceleration Mössbauer spectrometer (Jing et al. 1992) with a Rh matrix ^{57}Co source and a standard α-Fe foil for calibration. Data were collected over 512 channels, which on folding resulted in 256 channels. Spectra were accumulated to a low statistical uncertainty (typically 4–20×10^6 counts per channel) as an aid to attaining high-quality fits to the spectra as outlined below. A powdered quantity of each glass was distributed evenly in an approximately circular shape of diameter ~1.2 cm, such that the dimensionless absorber thickness was approximately 2, which corresponds to ~5 mg unenriched Fe/cm^2. The 4.2 K measurements were carried out using a standard tailed He bath cryostat. The isomer shift values are quoted relative to the centre of the RT α-Fe spectrum. The fraction of each phase was estimated from the area of the established components, assuming the same recoil-free fraction for ^{57}Fe in all samples. This assumption is supported by the similarity of results for those samples for which spectra were recorded at both RT and 4.2 K.

RESULTS

A total of 17 samples with 1% Fe_2O_3 were studied, from fully reduced ($\log f_{O_2} = -12.9$) to fully oxidized ($\log f_{O_2} = 4.8$). A series of Mössbauer-effect measurements were carried out on all of the samples at RT, with six samples selected across the full oxygen fugacity range ($\log f_{O_2} = -12.9$ to $+4.8$) for investigation at 4.2 K. The RT and 4.2 K Mössbauer spectra of representative samples are shown in Figures 1 and 2 respectively. The ^{57}Fe Mössbauer spectra of these disordered silicate samples containing Fe^{3+} and/or Fe^{2+} are different from the comparable paramagnetic spectra of crystalline materials, which generally reveal a more symmetric line shape and smaller line widths. As shown in Figure 1a, the cumulative absorption envelope of the fully reduced (Fe^{2+}) sample is distinctly asymmetric; the low-velocity component is more intense and has a smaller half width than the high-velocity component. As the oxygen fugacity increases, the resonance absorption between the asymmetric quadrupole-split doublet increases, the intensity of the high-velocity component of the asymmetric doublet decreases, and a tail region appears that constitutes a broadened magnetic sextet. These features indicate that as the oxygen fugacity increases, a second quadrupole-split doublet, whose low-velocity component coincides with that of the first doublet, appears in addition to a broadened magnetic sextet. The spectra of the fully oxidized sample (Figs. 1f and 2f) show only a broadened sextet and a more symmetric doublet with smaller isomer shift (IS) and quadrupole splitting (QS) values compared with the values of the doublets of the reduced sample. The asymmetric quadrupole doublet-like feature, which was the main feature in the spectrum of the reduced sample (Fig. 1a), no longer occurs in the spectrum of the oxidized sample (Fig. 1f).

A further 15 samples were studied with $Fe_2O_3 > 1$ wt%. Samples were prepared at $\log f_{O_2} = ~0$, -4, and -7, with Fe_2O_3 contents ranging from 2 to 30 wt%. These values of $\log f_{O_2}$ provide relatively oxidized, intermediate, and reduced samples containing significant amounts of both Fe^{2+} and Fe^{3+} in order to investigate and differentiate between possible Fe-Fe interactions. The spectrum of the sample prepared at $\log f_{O_2} \sim 0$ with 1 wt% Fe_2O_3 shown in Figure 1e is reproduced in Figure 3a. The cumulative absorption envelope of this sample consists of two broadened doublets and a tail region that constitutes a broadened magnetic sextet. As the Fe concentration increases (Figs. 3b–f), the area of the tail region decreases while the area of the symmetric doublet increases. The broadened sextet is absent from the spectra of all samples with ≥ 10 wt% Fe_2O_3. Similar spectra were obtained (not shown) for the samples prepared at $\log f_{O_2} \sim -4.0$ and -7.0 with Fe_2O_3 ranging from 2 to 30 wt%.
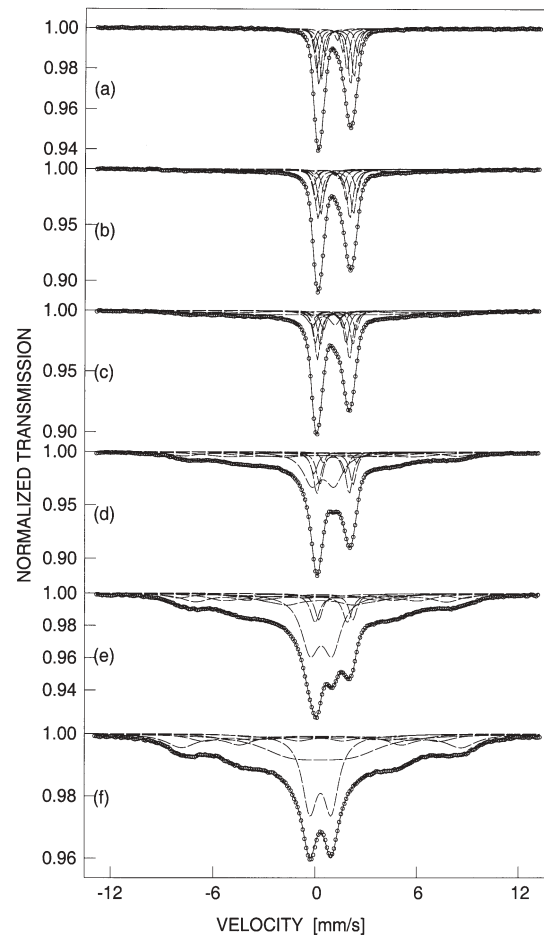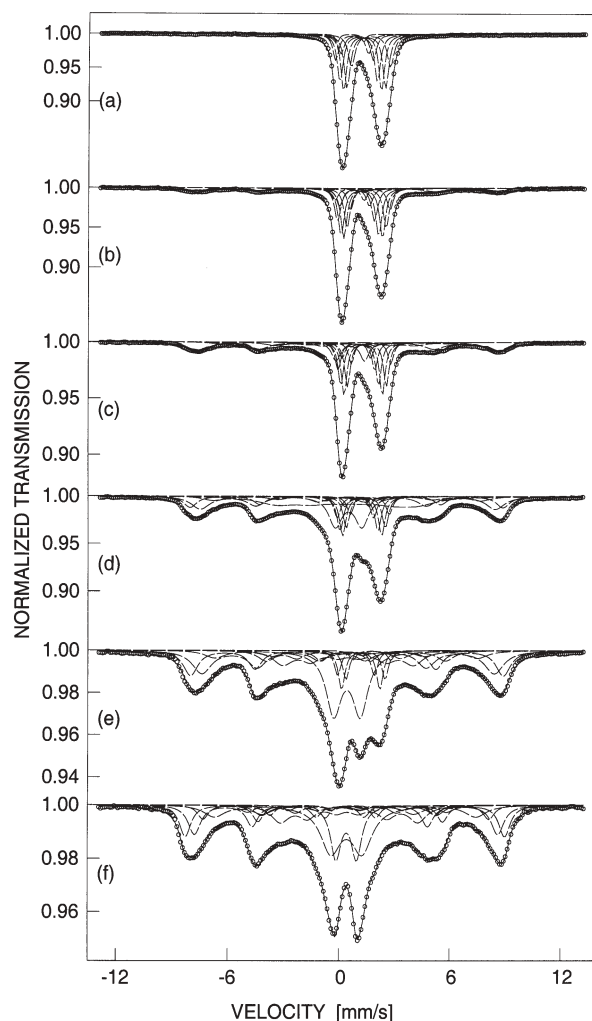

FIGURE 1. Room-temperature Mössbauer spectra of $AD_{eu} + ~1wt\%$ FeO_T glasses quenched from melts equilibrated at 1409 °C and $\log f_{O_2}$ values of: (**a**) -12.9, (**b**) -5.91, (**c**) -3.91, (**d**) -1.98, (**e**) -0.01 and (**f**) $+4.8$. Fits to the spectra were obtained using a set of symmetric Lorentzian doublets either without or with a set of symmetric Lorentzian sextets (method A, as discussed in the text; see also Fig. 4a).

Spectral analysis

Mössbauer spectroscopy was used in this study to determine $Fe^{3+}/\Sigma Fe$ ratios, which were calculated from the areas of Fe^{3+} absorption relative to the total area. Corrections due to thickness effects are minimal for these samples, and the use of spectra collected at 4.2 K removes errors due to differences in the recoil-free fractions of Fe^{2+} and Fe^{3+}. Although there is a wide range of methods available for fitting distributed and overlapping Mössbauer spectra (e.g., Campbell and Aubertin 1989; Murad and Cashion 2004), detailed studies have shown that the determination of $Fe^{3+}/\Sigma Fe$ from relative areas is relatively insensitive to the fitting method (e.g., Virgo and Mysen 1985; Helgason et al. 1992; Wilke et al. 2002). This insensitivity arises primarily from the large difference in isomer shift between Fe^{2+} and Fe^{3+}, which enables their spectral contributions to be distinguished, even when they partially overlap.
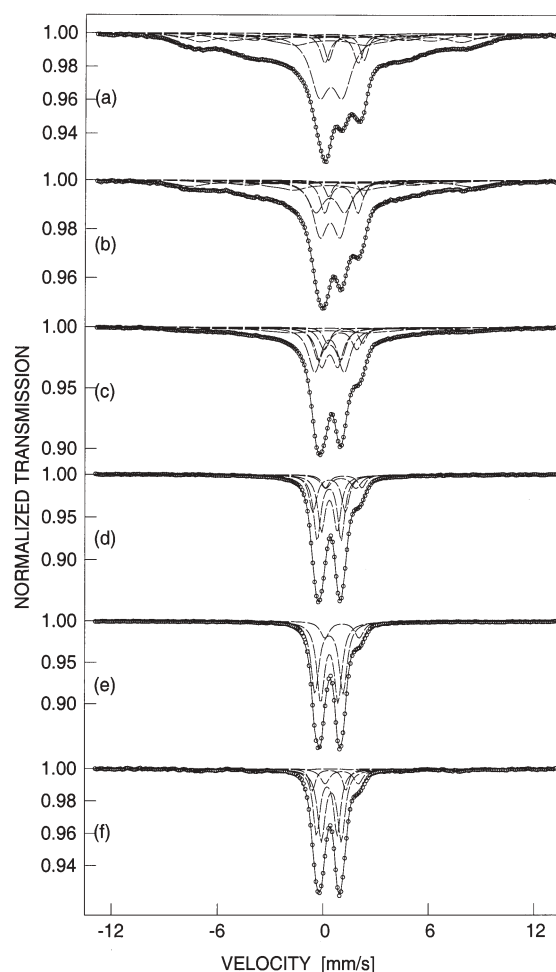
The ^{57}Fe Mössbauer spectrum of the highly reduced sample is dominated by an asymmetric broadened doublet (Fig. 1a) corre-

FIGURE 2. 4.2 K Mössbauer spectra of AD$_{eu}$ + ~ 1wt% FeO$_T$ glasses quenched from melts equilibrated at 1409 °C and log f_{O_2} values of: (**a**) –10.90, (**b**) –5.91, (**c**) –3.91, (**d**) –1.98, (**e**) –0.01 and (**f**) +4.8.

FIGURE 3. Room-temperature Mössbauer spectra of AD$_{eu}$ glasses quenched from melts equilibrated at 1409 °C and log f_{O_2} = –0.01 containing (**a**) ~ 1, (**b**) 1.75, (**c**) 3.67, (**d**) 9.81, (**e**) 18.75, and (**f**) 27.06, wt% FeO$_T$.

sponding to Fe²⁺ in a range of different environments. In order to develop a fitting method for Fe²⁺ absorption that could be applied to all spectra, two approaches were investigated to fit a spectrum of the same sample collected over a smaller velocity range. In the first method (method A; Fig. 4a), the different Fe²⁺ environments were modeled by a set of symmetric Lorentzian doublets with equal widths, whereas in the second method (method B; Fig. 4b), the different Fe²⁺ environments were modeled by a distribution of QS values using the program developed by Le Caër and Dubois (1979). The average value of $<QS>_B$ = 1.82 ± 0.02 mm/s obtained from this distribution fit (Fig. 4b) agrees well with the mean value of $<QS>_A$ = 1.84 ± 0.03 mm/s obtained from the computationally simpler fit using multiple symmetric Lorentzian doublets (Fig. 4a) (Table 2); hence, method A was chosen to fit all the other Mössbauer spectra.

The ⁵⁷Fe Mössbauer spectrum of the highly oxidized sample consists of a relatively symmetric quadrupole doublet combined with a highly broadened magnetic sub-spectrum (Fig. 1f). The IS of the quadrupole doublet (~0.33 mm/s) is significantly less than

TABLE 2. Parameters estimated from the analysis of the room temperature (RT) ⁵⁷Fe Mössbauer spectra of the reduced (FeV19) and oxidized (D60) samples (Figs. 1a and 1f, respectively)

Sample	log f_{O_2}	IS (mm/s)	QS (mm/s)	B$_{hf}$ (T)	Area%
FeV19	–12.9	1.444(5)	1.952(4)	–	11.2(1)
(Method A)		1.248(5)	1.923(2)	–	21.5(2)
		1.070(4)	1.893(2)	–	26.4(3)
		0.900(5)	1.812(4)	–	22.2(2)
		0.715(7)	1.697(6)	–	12.0(1)
		0.525(7)	1.438(6)	–	6.5(1)
		<IS>=1.03(4)	*<QS>=1.84(3)*	–	
FeV19	–12.9	*<IS>=1.02(1)*	*<QS>=1.82(2)*	–	
(Method B)					
D60	+4.8	0.331(3)	1.266(5)	–	27.4(3)
(Method A)		0.354(3)	0.026(5)	51.1(2)	20.7(2)
		0.354(3)	0.026(5)	43.0(2)	10.8(1)
		0.354(3)	0.026(5)	33.1(2)	9.1(1)
		0.354(3)	0.026(5)	25.5(2)	5.0(1)
		0.354(3)	0.026(5)	14.3(2)	26.7(3)
				<B$_{hf}$>= 32.3(2)	

Notes: Two methods (A and B) were used for the reduced sample, as described in the text. IS, QS, and B$_{hf}$ are isomer shift, quadrupole splitting, and hyperfine field, respectively. IS is measured relative to the center of the α-Fe spectrum at RT.

the value for the Fe^{2+} doublet in Figure 1a (~1.06 mm/s), and falls into the range observed for Fe^{3+} compounds (Burns and Solberg 1990). The magnetic spectrum arises from spin-spin relaxation times for Fe^{3+} that are slower than the characteristic measurement time of the Mössbauer transition (~10^{-8} s for ^{57}Fe), such that the time-averaged hyperfine field is no longer zero. Such relaxation effects are well known for dilute amorphous systems such as Fe^{3+}-doped silicate glasses, where Fe^{3+} atoms are simply too far apart to interact appreciably (Wickman 1966). Atomic relaxation times can be lengthened further by reducing the temperature, which ultimately results in an essentially static magnetic field at the nucleus and partly overlapped six-line magnetic spectra (Fig. 2f). The spectrum of the oxidized sample was therefore fitted to a broad symmetric quadrupole doublet ($\Gamma = 1.06$ mm/s) and a set of broadened magnetic sextets with Lorentzian lineshape, where the IS and quadrupole interaction (ϵ) values of all sextets were constrained to be equal, since the fluctuating relaxation times affect primarily the hyperfine field values. The hyperfine parameters of all components fitted to the spectrum of the oxidized sample are listed in Table 2.

The spectral analysis of the highly reduced (nearly all Fe^{2+}) and highly oxidized (nearly all Fe^{3+}) samples therefore suggested the following fitting model: paramagnetic Fe^{2+} = set of symmetric Lorentzian doublets with equal linewidths; paramagnetic Fe^{3+} =

symmetric Lorentzian doublet; magnetic Fe^{3+} = set of symmetric Lorentzian sextets with equal linewidths, IS, and ϵ values. All of the RT and 4.2 K spectra were fitted using the parameters obtained for either the highly reduced or the highly oxidized sample as starting values, and the fits obtained for selected spectra are shown in Figures 1 and 2. The mean value of each hyperfine parameter is relatively independent of the fitting model (e.g., Virgo and Mysen 1985), and was calculated by averaging the parameter values weighted by the corresponding subspectral areas of Fe^{2+} or Fe^{3+} components. The mean hyperfine parameters as well as the subspectral area values are listed in Table 3.

The <IS> and <QS> values at RT and 4.2 K for Fe^{2+} and Fe^{3+} show consistent trends, with values at 4.2 K higher than those at RT according to expected behavior (e.g., Murad and Cashion 2004) (Fig. 5). The consistent variation of both the <IS> and <QS> values as a function of Fe^{3+}/ΣFe further supports the correct separation and identification of the Fe^{2+} and Fe^{3+} contributions in the spectral fitting. The good agreement between the Fe^{2+} and Fe^{3+} areas determined from the fits to the RT and 4.2 K spectra supports the assumption that the recoil-free fractions of Fe^{2+} and Fe^{3+} are approximately equal.

The mean hyperfine parameter values provide an indication of Fe coordination in the glass. The <IS> values of Fe^{3+} are almost constant for Fe^{3+}/ΣFe < 0.65 (IS$_{RT}$ ≈ 0.46 mm/s and IS$_{4.2 K}$ ≈ 0.51 mm/s), and decrease to <IS>$_{RT}$ ≈ 0.33 mm/s and <IS>$_{4.2 K}$ ≈ 0.42 mm/s for the fully oxidized sample. This may indicate a change from octahedral coordination in reduced glasses to tetrahedral coordination in oxidized glasses, similar to the observation of Virgo and Mysen (1985) and Mysen et al. (1985b) for CaO-SiO$_2$-Al$_2$O$_3$-Fe$_2$O$_3$ and MgO-SiO$_2$-Al$_2$O$_3$-Fe$_2$O$_3$ glasses. The IS,
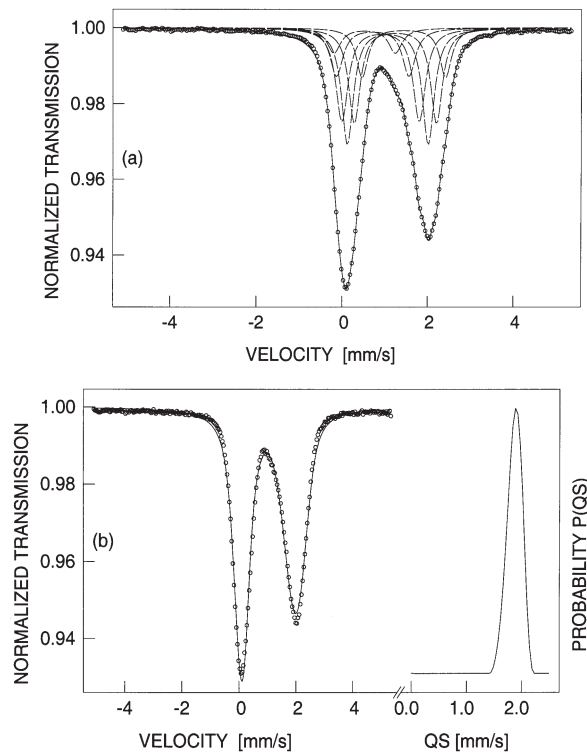
FIGURE 4. Room-temperature Mössbauer spectrum of the ~1 wt% FeO$_T$ glass synthesized at log f_{O_2} = 12.9 (as in Fig. 1a). The spectrum was fitted using methods A and B as discussed in the text. **(a)** Method A = a set of elementary doublets of Lorentzian shape with $\Gamma = 0.31$ mm/s. **(b)** Method B = fit to a distribution of quadrupole splittings using the program of Le Caër and Dubois (1979). The corresponding probability distribution curve P(QS) is also shown.
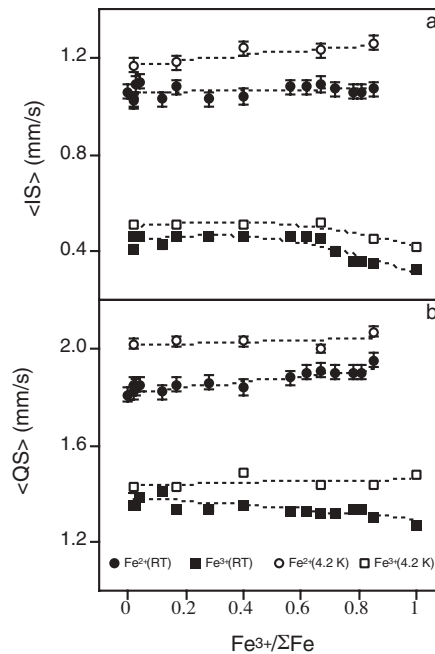
FIGURE 5. Plot of the **(a)** average isomer shift (<IS>) and **(b)** average quadrupole splitting (<QS>), of Fe^{2+} and Fe^{3+} at RT and 4.2 K as a function of Fe^{3+}/ΣFe for melts equilibrated from –12.9 to +4.8. The dotted lines indicate the trends of the data and act as a guide to the eye.

TABLE 3. Parameters estimated from the analysis of the room temperature (RT) and 4.2 K ^{57}Fe Mössbauer spectra of the silicate glasses using fitting method A

log f_{O_2}	Fe³⁺/Σ Fe	Fe²⁺ doublet			Fe³⁺ doublet			Fe³⁺ sextet			
		<IS> mm/s	<QS> mm/s	Area %	<IS> mm/s	<QS> mm/s	Area %	IS mm/s	ε mm/s	B_{hf}^{max} T	Area %
Room	Temperature										
-12.9	0	1.06(3)	1.81(3)	100			0				0
-10.9	0.025	1.03(3)	1.85(3)	97.5	0.46(1)	1.35(1)	2.5				0
-9.91	0.022	1.02(3)	1.82(3)	97.8	0.41(1)	1.42(1)	2.2				0
-8.90	0.030	1.09(3)	1.84(3)	97.0	0.46(1)	1.35(1)	3.0				0
-7.88	0.043	1.10(3)	1.85(3)	95.7	0.46(1)	1.39(1)	4.3				0
-6.91	0.120	1.03(3)	1.82(3)	88.0	0.43(1)	1.41(1)	2.8	0.36(2)	0.026(5)	43.1(2)	9.2
-5.91	0.171	1.08(3)	1.85(3)	82.9	0.46(1)	1.34(1)	3.1	0.34(2)	0.026(5)	46.6(2)	14.0
-4.91	0.280	1.03(3)	1.86(3)	72.0	0.46(1)	1.34(1)	5.4	0.32(2)	0.026(5)	48.8(2)	22.6
-3.91	0.399	1.04(3)	1.84(3)	60.1	0.46(1)	1.35(1)	9.1	0.34(2)	0.026(5)	47.3(2)	30.8
-3.01	0.558	1.08(3)	1.88(3)	44.2	0.46(1)	1.33(1)	16.5	0.34(2)	0.026(5)	48.2(2)	39.3
-2.42	0.624	1.08(3)	1.90(3)	37.6	0.46(1)	1.33(1)	20.7	0.34(2)	0.026(5)	50.1(2)	41.7
-1.98	0.667	1.09(3)	1.91(3)	33.3	0.45(1)	1.32(1)	24.0	0.33(2)	0.026(5)	50.0(2)	42.7
-1.50	0.717	1.07(3)	1.90(3)	28.3	0.40(1)	1.32(1)	25.6	0.34(2)	0.026(5)	49.0(2)	46.1
-1.01	0.784	1.06(3)	1.90(3)	21.6	0.36(1)	1.34(1)	29.0	0.33(2)	0.026(5)	50.4(2)	49.4
-0.69	0.807	1.06(3)	1.90(3)	19.3	0.36(1)	1.34(1)	28.3	0.32(2)	0.026(5)	52.2(2)	52.5
-0.01	0.851	1.07(3)	1.95(3)	14.9	0.35(1)	1.30(1)	30.9	0.33(2)	0.026(5)	52.0(2)	54.2
+4.8	1.00			0	0.33(1)	1.27(1)	27.4	0.35(2)	0.026(5)	51.1(2)	72.6
4.2 K											
-10.90	0.021	1.17(3)	2.02(3)	97.9	0.51(1)	1.43(1)	2.1				0
-5.91	0.182	1.18(3)	2.03(3)	81.8	0.51(1)	1.43(1)	4.3	0.37(2)	0.032(5)	50.4(2)	13.9
-3.91	0.389	1.24(3)	2.03(3)	61.1	0.51(1)	1.49(1)	8.5	0.42(2)	0.032(5)	50.6(2)	30.4
-1.98	0.657	1.23(3)	2.00(3)	34.4	0.52(1)	1.44(1)	13.5	0.49(2)	0.035(5)	52.4(2)	52.1
-0.01	0.849	1.24(3)	2.07(3)	15.1	0.45(1)	1.44(1)	21.5	0.45(2)	0.035(5)	52.5(2)	63.4
+4.8	1.00			0	0.42(1)	1.48(1)	30.5	0.40(2)	0.040(5)	53.6(2)	69.5

Notes: <IS> and <QS> are the average values weighted by areas. IS is relative to the center of the α-Fe spectrum at RT. The estimated error is given in brackets. B_{hf}^{max} is the maximum value of the hyperfine field obtained.

QS, and hyperfine field (B_{hf}) values of the Fe³⁺ sextets are in the ranges $IS_{RT} = (0.32–0.36)$ mm/s, $IS_{4.2K} = (0.37–0.49)$ mm/s, $QS_{RT} = 0.026$ mm/s, $QS_{4.2K} = 0.035$ mm/s, $B_{hf\,RT} = (43.0–52.2)$ T, and $B_{hf\,4.2K} = (50.4–53.6)$ T, which suggest tetrahedral coordination. The average hyperfine parameter values obtained for the Fe²⁺ doublet are in the ranges $<IS>_{RT} = (1.02–1.10)$ mm/s, $<QS>_{RT} = (1.81–1.95)$ mm/s, $<IS>_{4.2K} = (1.17–1.26)$ mm/s, and $<QS>_{4.2K} = (2.02–2.07)$ mm/s. These values are intermediate between those values normally attributable to tetrahedrally and octahedrally coordinated Fe²⁺ and may represent a range of coordination environments (Burns and Solberg 1990).

The RT ^{57}Fe Mössbauer spectra of the silicate glasses prepared at $f_{O_2} \sim 0.0$, –4.0, and –7.0 with 2–30 wt% Fe₂O₃ were fitted using the same fitting model as the spectra for the 1 wt% Fe₂O₃ samples. The fits obtained for selected spectra are shown in Figure 3, and the values of the hyperfine parameters are summarized in Table 4.

Thermodynamic evaluation

The ratio of Fe²⁺ to Fe³⁺ in a silicate melt can be represented by the reaction:

$$\text{Fe}^{2+}\text{O} + 1/4\,\text{O}_2 = \text{Fe}^{3+}\text{O}_{1.5} \qquad (1)$$
silicate melt   silicate melt

Therefore, at equilibrium:

$$\ln\left(\frac{X_{\text{Fe}^{3+}\text{O}_{1.5}}}{X_{\text{Fe}^{2+}\text{O}}}\right) = \frac{-\Delta G_r^0(1)}{RT} - \ln\left(\frac{\gamma_{\text{Fe}^{3+}\text{O}_{1.5}}}{\gamma_{\text{Fe}^{2+}\text{O}}}\right) + \frac{1}{4}\ln f_{O_2} \qquad (2)$$

where ΔG_r^0 (1) corresponds to ΔG_r^0 of Reaction 1, and $\gamma_{\text{Fe}^{3+}\text{O}_{1.5}}$ and $\gamma_{\text{Fe}^{2+}\text{O}}$ are the activity coefficients of Fe³⁺O₁.₅ and Fe²⁺O in

the silicate melt, referenced to the standard states of pure liquid Fe³⁺O₁.₅ and Fe²⁺O, respectively, at the temperature and pressure of interest.

As the total Fe dissolved in the silicate melt approaches infinite dilution, not only should the behavior of both the Fe³⁺O₁.₅ and Fe²⁺O components obey Henry's law (in which the activity coefficient of a component becomes independent of its own concentration), but also the interaction between the Fe³⁺O₁.₅ and Fe²⁺O components should approach zero; that is, both $\gamma_{\text{Fe}^{3+}\text{O}_{1.5}}$ and $\gamma_{\text{Fe}^{2+}\text{O}}$ should be constant (at constant temperature and pressure) at all Fe³⁺/Fe²⁺ ratios. These Henry's law activity coefficients (at infinite dilution) will be represented as $\gamma_{\text{Fe}^{3+}\text{O}_{1.5}}^{\infty}$ and $\gamma_{\text{Fe}^{2+}\text{O}}^{\infty}$, respectively. If we assume that our experiments with 1 wt% Fe₂O₃ (nominal) are sufficiently close to the theoretical state of infinite dilution, regression of $\ln(X_{\text{Fe}^{3+}\text{O}_{1.5}}/X_{\text{Fe}^{2+}\text{O}})$ against $\ln f_{O_2}$ should then give a line of slope 1/4 with an intercept of $[-\Delta G_r^0 (1)/RT - \ln (\gamma_{\text{Fe}^{3+}\text{O}_{1.5}}^{\infty}$ and $\gamma_{\text{Fe}^{2+}\text{O}}^{\infty})]$.

The data between $\log f_{O_2} = -13$ and 0 at ~1% FeO_T (16 data) were fitted by weighted non-linear least-squares regression to this equation. We used the uncertainties in $\log f_{O_2}$ given in Table 1. The uncertainty in Fe³⁺/ΣFe is difficult to estimate a priori, as Fe³⁺ and Fe²⁺ are each obtained by summing the areas under several doublets, the fits to which are highly correlated with each other. Consequently, the uncertainty was estimated externally from the reproducibility of the data, by requiring the reduced chi-squared (χ_v^2) for the regression to be near unity. We find that $\sigma(\text{Fe}^{3+}/\Sigma\text{Fe})$ is 0.01.

To test the model, we first performed the regression allowing the exponent to vary. As shown in Figure 6, we obtained an exponent of 0.245 ± 0.004, with $\chi_v^2 = 1.21$. The value of the exponent is thus confirmed to be insignificantly different from the theoretical expectation of 0.25. If we repeat the regression

TABLE 4. Parameters estimated from the analysis of the RT ^{57}Fe Mössbauer spectra of the AD_{eu} + FeO_{tot} silicate glasses prepared at log f_{O_2} ~ 0.0, −4.0 and −7.0 with FeO_T > 1 wt%

Sample	log f_{O_2}	FeO$_T$ wt%	X_{FeO_T}	Fe²⁺ doublet <IS> mm/s	<QS> mm/s	Area %	Fe³⁺ doublet <IS> mm/s	<QS> mm/s	Area %	Fe³⁺ sextet IS mm/s	ε mm/s	B$_{hf}$^{max} T	Area %	Fe³⁺/ΣFe
D31/7/01	−0.01	1.75(3)	0.0134(2)	1.05(3)	1.93(3)	15.3	0.34(2)	1.34(2)	42.6	0.33(2)	0.025(5)	49.7(2)	42.0	0.846
		3.67(7)	0.0282(6)	1.04(3)	1.92(3)	16.8	0.33(2)	1.36(2)	57.9	0.33(2)	0.025(5)	50.0(2)	25.3	0.832
		6.44(13)	0.0494(10)	1.06(3)	1.93(3)	15.8	0.32(2)	1.34(2)	76.3	0.33(2)	0.025(5)	38.0(2)	7.9	0.842
		9.81(6)	0.0766(5)	1.05(3)	1.88(3)	17.4	0.33(2)	1.33(2)	82.6					0.826
		18.75(12)	0.1498(11)	0.98(3)	1.76(3)	18.1	0.32(2)	1.29(2)	81.9					0.819
		27.06(11)	0.2201(9)	0.95(3)	1.68(3)	17.5	0.33(2)	1.25(2)	82.5					0.825
C14/12/01	−3.91	1.49(6)	0.0114(4)	1.04(3)	1.84(2)	61.6	0.42(1)	1.36(1)	14.5	0.32(2)	0.024(5)	49.0(5)	23.9	0.384
		2.79(9)	0.0214(7)	1.02(3)	1.83(2)	62.5	0.34(1)	1.30(1)	20.2	0.32(2)	0.024(5)	50.0(5)	17.4	0.375
		5.36(9)	0.0414(7)	1.03(3)	1.85(2)	64.9	0.33(1)	1.31(1)	30.7	0.32(2)	0.024(5)	43.0(5)	4.4	0.351
		7.96(13)	0.0620(10)	1.03(3)	1.84(2)	65.2	0.30(1)	1.32(1)	33.0	0.32(2)	0.024(5)	39.3(5)	1.8	0.348
		16.36(11)	0.1298(9)	1.02(3)	1.84(2)	62.4	0.29(1)	1.12(1)	37.6					0.376
C27/11/01	−6.91	3.52(10)	0.0271(8)	1.02(3)	1.83(2)	89.8	0.42(1)	1.38(1)	7.2	0.36(2)	0.024(5)	28.2(5)	3.0	0.102
		5.83(7)	0.0451(6)	1.02(3)	1.84(2)	91.0	0.35(1)	1.33(1)	9.1					0.091
		7.96(9)	0.0619(7)	1.02(3)	1.84(2)	91.3	0.33(1)	1.33(1)	8.7					0.087
		26.82(13)	0.2186(11)	1.04(3)	1.85(2)	79.2	0.34(1)	1.36(1)	21.8					0.218

Notes: <IS> and <QS> are the average values weighted by area. IS is relative to the centre of the α-Fe spectrum at RT. The estimated error is given in brackets. B$_{hf}$^{max} is the maximum value of the hyperfine field. Areas are for the subspectra of Fe²⁺ and Fe³⁺ sites.

fixing the exponent at 0.25 exactly, then $\chi_v^2 = 1.24$, with the constant in the regression $[-\Delta G_r^0 (1)/RT - \ln (\gamma_{Fe^{3+}O_{1.5}}^\infty$ and $\gamma_{Fe^{2+}O}^\infty)]$ = 1.861 ± 0.017.

The experimental precision of $\sigma(Fe^{3+}/\Sigma Fe) = 0.01$ is a robust result: because $\sigma(Fe^{3+}/\Sigma Fe) \gg \sigma (\log f_{O_2})$ relatively, doubling $\sigma(Fe^{3+}/\Sigma Fe)$ has the effect of nearly doubling χ_v^2. This precision is better than that usually quoted for determinations of $Fe^{3+}/\Sigma Fe$ by Mössbauer spectroscopy, where the uncertainty is typically given as ~3–5% (e.g., Mysen et al. 1985a, 1985b; Dyar et al. 1987). The consistent variation of Fe^{3+} concentration with f_{O_2} is also likely to be related to the identical nature of the samples in all respects apart from the f_{O_2} of preparation. For example, Dyar et al. (1987) have shown that the method used to quench experimental glasses can affect Mössbauer spectra; here, the use of the same quenching procedure for all glasses eliminates this variable.

Whereas the precision of a series of measurements can be assessed by statistical examination, their accuracy is appropriately viewed as an hypothesis, whose merits are assessed through its survival of tests aimed at its falsification (Popper 1963). Here, the hypothesis that our $Fe^{3+}/\Sigma Fe$ measurements on the samples with 1 wt% FeO_T are accurate may be assessed against the following tests:

(1)   Results of $Fe^{3+}/\Sigma Fe$ determinations at RT are in good agreement with those at 4.2 K on the same sample (Fig. 6), despite the very different appearance of the spectra. These data rule out the speculation that there might be a significant difference in the recoil-free fractions of Fe^{3+} and Fe^{2+} in silicate glasses, at least for the composition studied here.

(2)   The slope of $\ln(X_{Fe^{3+}O_{1.5}}/X_{Fe^{2+}O})$ versus $\ln f_{O_2}$ is within uncertainty of the theoretically expected value of 0.25.

(3)   The results conform well with the expectation that $Fe^{3+}/\Sigma Fe \to 0$ at very low f_{O_2} and $Fe^{3+}/\Sigma Fe \to 1$ at very high f_{O_2}.

This last criterion provides a robust test of any method of determining $Fe^{3+}/\Sigma Fe$ ratios but has not to the best of our knowledge been used previously, e.g., to test wet-chemical protocols. This may be due to the difficulty of synthesizing glasses with $Fe^{3+}/\Sigma Fe = 1$, which requires high-pressure methods for geologically relevant compositions.

We do not suggest that either the precision or accuracy
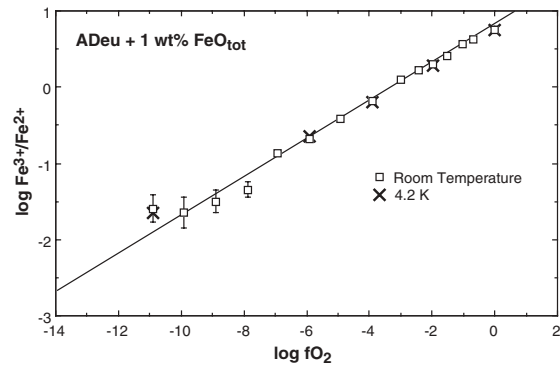
FIGURE 6. The relationship between log (Fe^{3+}/Fe^{2+}) and log f_{O_2} for the ~ 1wt% FeO_T. The solid line of slope $m = 0.245 \pm 0.004$ is the weighted linear fit to all the room temperature (RT) data points (except that at log f_{O_2} = +4.8). Error bars, which are shown where they are larger than the symbols, are one standard deviation, propagated assuming that the uncertainty in $Fe^{3+}/\Sigma Fe$ is ±0.01, as discussed in the text.

claimed here for $Fe^{3+}/\Sigma Fe$ determined by Mössbauer spectroscopy on this carefully prepared series of experimental samples is applicable to natural silicate glasses, where other variables such as different cooling rates may complicate the interpretation of Mössbauer spectra. An additional benefit of the accuracy with which $Fe^{3+}/\Sigma Fe$ has been determined in these samples is that they make excellent calibration standards for XANES spectroscopy (Berry et al. 2003).

A hypothetical alternative thermodynamic formulation of Reaction 1 might be to use $X_{Fe_2^{3+}O_3}$ as the mole fraction of the Fe^{3+} component, in which case the reaction would be written as:

$$2Fe^{2+}O + 1/2\ O_2 = Fe_2^{3+}O_3 \tag{1a}$$
silicate melt   silicate melt

which, since ΔG_r^0 (1a) = $2\Delta G_r^0$ (1), leads to the equation:

$$\ln\left(\frac{X_{Fe_2^{3+}O_3}}{(X_{Fe^{2+}O})^2}\right) = \frac{-2\Delta G_r^0(1)}{RT} - \ln\left(\frac{\gamma_{Fe_2^{3+}O_3}}{(\gamma_{Fe^{2+}O})^2}\right) + \frac{1}{2}\ln f_{O_2} \tag{3}$$

Regression of $\ln[X_{Fe_2^{3+}O_3}/(X_{Fe^{2+}O})^2]$ vs. $\ln f_{O_2}$ should give a line of slope 1/2, which may be tested empirically. We find that the fit to the data is poor, with $\chi_v^2 = 3.37$ when the input data are weighted exactly as for the first fit (which gave $\chi_v^2 = 1.21$), and the slope comes out at 0.350 ± 0.005, which is inconsistent with the starting assumption regarding the stoichiometry of Reaction 1a. Our results therefore show unambiguously that the hypothesis that Fe³⁺ occurs in silicate melts as the Fe³⁺-Fe³⁺ dimer, as is implied by using $X_{Fe_2^{3+}O_3}$ as the mole fraction, is an extremely poor one.

Reaction 1 may be thought of as the difference between the two reactions:

$$\text{Fe} + 3/4\,O_2 = \text{Fe}^{3+}O_{1.5} \qquad (4)$$
metal \qquad\qquad silicate melt

$$\text{Fe} + 1/2\,O_2 = \text{Fe}^{2+}O \qquad (5)$$
metal \qquad\qquad silicate melt

Therefore, $\Delta G_r^0(1) = \Delta G_r^0(4) - \Delta G_r^0(5)$. The Gibbs free energy of Reaction 5 has been given as (O'Neill and Eggins 2002):

$$\Delta G_r^0(5) \text{ (J/mol)} = -244118 + 115.559\,T - 8.474\,T \ln T$$

and using this expression, O'Neill and Eggins (2002) obtained, by equilibration with Fe metal under controlled f_{O_2}, $\gamma_{Fe^{2+}O}^\circ = 1.37 \pm 0.01$ for the AD_{eu} composition at 1673 K and 1 bar.

Unfortunately, equivalent thermodynamic data for Reaction 4 are less certain, as little is known of the thermodynamic properties of molten Fe₂O₃. The reason for this lack of knowledge is that Fe₂O₃ reduces to Fe₃O₄ at 1730 K in pure O₂ at 1.013 bars (Wriedt 1991). Consequently, studying the melting behavior of Fe₂O₃ would require $f_{O_2} \gg 1$ bar, which is difficult experimentally. Nevertheless, thermodynamic data of useful accuracy may be estimated as follows. The free energy of the reaction:

$$\text{Fe} + 1/2O_2 = \text{Fe}^{3+}O_{1.5} \qquad (4a)$$
metal \qquad\qquad corundum

is taken from Robie and Hemingway (1995) as:

$$\Delta G_r^0 \text{ (4a) (J/mol)} = -411565 + 167.095\,T - 5.350\,T \ln T$$

Phillips and Muan (1960) studied melting relations in the system Fe₃O₄-Fe₂O₃ to 45 atm O₂. Extrapolation of their rather limited data on the liquidus at the Fe₂O₃-rich side of the phase diagram suggests a melting point for Fe₂O₃ that is at least greater than 1900 K. We adopt 2100 K, with a likely error of ±200 K. The entropies of melting (ΔS_m^0) of some other corundum-structured oxides are 24.9 J/(K·mol) for CrO₁.₅ and 23.9 J/(K·mol) for AlO₁.₅ (Barin et al. 1989). We therefore adopt 24.5 J/(K·mol) for ΔS_m^0 of Fe³⁺O₁.₅. With this value and $T_M = 2100$ K, the free energy of melting is approximately:

$$\Delta G_m^0 (\text{Fe}^{3+}O_{1.5}) \text{ (J/mol)} = 24.5(T - 2100)$$

Therefore:

$$\Delta G_r^0 (4) \text{ (J/mol)} = -360115 + 142.595\,T - 5.350\,T \ln T$$

Hence:

$$\Delta G_r^0(1) \text{ (J/mol)} = -115997 + 27.036\,T + 3.124\,T \ln T$$

The uncertainty in $\Delta G_r^0(1)$ is about ±5 kJ/mol, based on quoted uncertainties for $\Delta G_r^0(5)$ of ±0.3 kJ/mol (O'Neill and Eggins 2002), in $\Delta G_r^0(4a)$ of 0.7 kJ/mol (Robie and Hemingway 1995), and reasonable uncertainties in ΔS_m^0 and T_m for Fe³⁺O₁.₅ of 5 J/(K·mol) and 200 K, respectively. It is the latter that predominates. At 1682 K, $\Delta G_r^0(1)/RT = -2.25 \pm 0.36$. Combining this with the result of the regression analysis of our data and $\gamma_{Fe^{2+}O}^\circ = 1.37$, we obtain $\gamma_{Fe^{3+}O_{1.5}}^\circ = 1.08 \pm 0.33$, implying that solution of Fe³⁺O₁.₅ in AD_{eu} melt is close to ideal.

Effects of adding FeO$_T$

Because both $\gamma_{Fe^{2+}O}^\circ$ and $\gamma_{Fe^{3+}O_{1.5}}^\circ$ differ from unity, adding FeO$_T$ to the system must change Fe³⁺/ΣFe slightly, because, by definition, both $\gamma_{Fe^{2+}O} \to 1$ and $\gamma_{Fe^{3+}O_{1.5}} \to 1$ as $X_{Fe^{2+}O}$ and $X_{Fe^{3+}O_{1.5}} \to 1$, respectively. However, a potentially larger effect might be obtained if there are significant Fe³⁺-Fe²⁺ interactions in silicate melts, as suggested by Kress and Carmichael (1988) to explain the non-ideal value of the exponent. To test this hypothesis, we investigated the effect of adding increasing amounts of FeO$_T$ to the AD_{eu} composition. The results are presented in Table 4 and plotted in Figure 7. The uncertainties in Fe³⁺/ΣFe for these higher FeO$_T$ samples are somewhat larger than for the 1% FeO$_T$ samples, as the change in the nature of the Mössbauer spectra with increasing FeO$_T$ means that the fits to the 1% FeO$_T$ series do not serve as good guides to the fitting procedure. Also, we have no means of obtaining an independent external estimate of $\sigma(\text{Fe}^{3+}/\Sigma\text{Fe})$ for these samples in the way that we estimated the uncertainty in the 1% FeO$_T$ samples from their scatter about the fit to Equation 2. Accordingly, we estimated that $\sigma(\text{Fe}^{3+}/\Sigma\text{Fe}) = 0.02$ for all samples with FeO$_T > 1\%$, based on the statistics of the fitting procedure. Clearly, Fe³⁺/ΣFe changes with increasing FeO$_T$ by amounts substantially greater than this uncertainty, in all three compositions.

The variation of Fe³⁺/ΣFe with FeO$_T$ may be explained by non-ideal interactions in the silicate melt, as follows. Following the approach suggested by Sack et al. (1980), but not actually used by them (see discussion in later section), we used the simplest way to describe deviations from ideality in a multi-component solution, namely, the regular solution model. In this model, the excess free energy of mixing, G_{ex}, is given by:

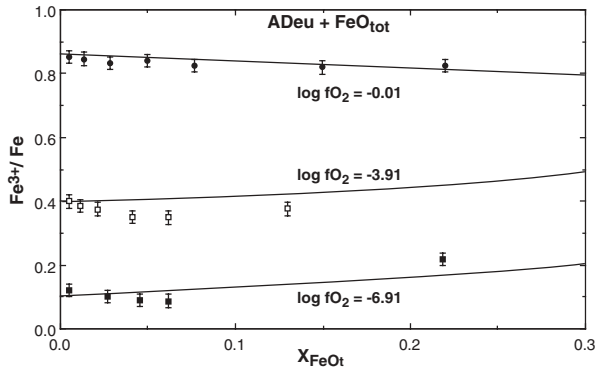$$G_{ex} = \sum_{i=1}^{n-1} \sum_{j>i}^{n} X_i X_j W_{i-j} \qquad (6)$$

where X_i and X_j are the mole fractions of the oxide components, here defined on the single-cation basis (e.g., X_{SiO_2}, $X_{AlO_{1.5}}$, $X_{Fe^{2+}O}$, $X_{Fe^{3+}O_{1.5}}$, etc., and W_{i-j} is the interaction or Margules parameter. Hence, activity coefficients are given by:

$$\ln \gamma_i = \sum_{j \neq i}^{n} X_j W_{i-j} / RT - G_{ex} \qquad (7)$$

When the ratio of two activity coefficients is taken, a relatively simple expression results:

$$\ln(\gamma_{Fe^{3+}O_{1.5}}/\gamma_{Fe^{2+}O}) =$$
$$\sum_{j}^{n} X_j(W_{Fe^{3+}-j} - W_{Fe^{2+}-j}) / RT + (X_{Fe^{2+}O} - X_{Fe^{3+}O_{1.5}})W_{Fe^{2+}-Fe^{3+}} / RT \qquad (8)$$

FIGURE 7. $Fe^{3+}/\Sigma Fe$ as a function of X_{FeO_T} in the system AD_{eu}-FeO_T. The curves are the best fits to Equation 10, with $\Delta G_r^0(1)/RT$ constrained at –2.25. Error bars are ±0.02 in $Fe^{3+}/\Sigma Fe$.

The term in $W_{Fe^{2+}-Fe^{3+}}$ describes the interactions between $Fe^{2+}O$ and $Fe^{3+}O_{1.5}$. For very low amounts of FeO_T, where $X_{Fe^{2+}O}$ and $X_{Fe^{3+}O_{1.5}}$ are both near zero, this term is obviously negligible. Now, when FeO_T is added to an FeO_T–free composition, the mole fractions X_j are given by:

$$X_j = X_j^0 (1 - X_{Fe^{2+}O} - X_{Fe^{3+}O_{1.5}}) \tag{9}$$

where X_j^0 are the mole fractions in the FeO_T–free composition. Substituting Equations 8 and 9 into 2 gives:

$$\ln\left(\frac{X_{Fe^{3+}O_{1.5}}}{X_{Fe^{2+}O}}\right) = \frac{-\Delta G_r^0(1)}{RT} - \ln(\gamma_{Fe^{3+}O_{1.5}}^\infty / \gamma_{Fe^{2+}O}^\infty)(1 - X_{Fe^{2+}O} - X_{Fe^{3+}O_{1.5}})$$
$$+ (X_{Fe^{2+}O} - X_{Fe^{3+}O_{1.5}})W_{Fe^{2+}-Fe^{3+}} / RT + \frac{1}{4}\ln f_{O_2} \tag{10}$$

This simple theory describes the effect of adding FeO_T using just one additional parameter (namely, $W_{Fe^{2+}-Fe^{3+}}/RT$) to that required to describe the system at low FeO_T values, although we also need to know the ratio ($\gamma_{Fe^{3+}O_{1.5}}^\infty / \gamma_{Fe^{2+}O}^\infty$), as this is not obtained independently of $\Delta G_r^0(1)$ from fitting the 1% FeO_T data.

Accordingly, we fitted simultaneously both the data at 1% FeO_T (Table 2) and at higher FeO_T concentrations (Table 4) to Equation 10, first constraining $\Delta G_r^0(1)/RT = -2.25$. This procedure gives a reasonable fit to the data, with $W_{Fe^{2+}-Fe^{3+}}/RT = -3.36$ ± 0.67, $\ln(\gamma_{Fe^{3+}O_{1.5}}^\infty / \gamma_{Fe^{2+}O}^\infty) = 0.97 \pm 0.04$, and $\chi_v^2 = 2.01$. Allowing $\Delta G_r^0(1)/RT$ to vary does not improve the fit at all ($\chi_v^2 = 2.03$); the value of $\Delta G_r^0(1)/RT$ refined by the regression becomes -1.79 ± 0.39, with $\ln(\gamma_{Fe^{3+}O_{1.5}}^\infty / \gamma_{Fe^{2+}O}^\infty) = -0.11 \pm 0.88$, while $W_{Fe^{2+}-Fe^{3+}}/RT$ remains unchanged at -3.35 ± 0.67. The $W_{Fe^{2+}-Fe^{3+}}$ value of -47.0 ± 9.4 kJ/mol (at 1682 K) represents a significant interaction, with the negative sign indicating a tendency toward the formation of a Fe^{2+}-Fe^{3+} complex in the melt. The magnitude of the term further allows us to test the assumption that we made initially in the fitting of our 1% FeO_T data, that both $\gamma_{Fe^{3+}O_{1.5}}$ and $\gamma_{Fe^{2+}O}$ should be constant (at constant temperature and pressure) at all Fe^{3+}/Fe^{2+} ratios. Now, 1% FeO_T corresponds to a combined mole fraction ($X_{Fe^{2+}O} + X_{Fe^{3+}O_{1.5}}$) of 0.0076. With $W_{Fe^{2+}-Fe^{3+}}/RT = -3.36$, it is easy to confirm that the magnitude of the term ($X_{Fe^{2+}O} - X_{Fe^{3+}O_{1.5}}$)$W_{Fe^{2+}-Fe^{3+}}/RT$ (cf., Eq. 8) then remains very much smaller than the

uncertainty in $\ln (X_{Fe^{3+}O_{1.5}})/(X_{Fe^{2+}O})$ at all values of $Fe^{3+}/\Sigma Fe$, assuming $\sigma(Fe^{3+})$ is 0.01.

This model, being based on the regular solution formalism, necessarily assumes that the interactions between Fe^{3+} and Fe^{2+} are symmetric as regards to composition (i.e., the interaction effects reach a maximum when $X_{Fe^{2+}O}/X_{Fe^{3+}O_{1.5}} = 1$). This restriction means that the model cannot adequately describe, for example, magnetite-like complexes where the interaction would be expected to reach a maximum at the magnetite stoichiometry, $X_{Fe^{2+}O}/X_{Fe^{3+}O_{1.5}} = 0.5$. However, incorporating asymmetric mixing terms greatly increases the complexity of the model, and we have not explored that possibility.

DISCUSSION

Over the last forty years, a substantial experimental effort has been put into measuring $Fe^{3+}/\Sigma Fe$ in silicate melts, both in simple systems and in more compositionally complex systems approximating natural magmas, with $Fe^{3+}/\Sigma Fe$ analyzed either by wet chemistry or Mössbauer spectroscopy, and occasionally by both methods. An important result of this effort has been the development of empirical equations relating $Fe^{3+}/\Sigma Fe$ to f_{O_2} and melt composition, such as those of Sack et al. (1980), Kilinc et al. (1983), and Kress and Carmichael (1991). These equations provide the means by which f_{O_2} in a natural magma is estimated if $Fe^{3+}/\Sigma Fe$ can be determined (e.g., Christie et al. 1986), or, if f_{O_2} is known or assumed, $Fe^{3+}/\Sigma Fe$ can be calculated where it has not been measured. The database underpinning these equations potentially comprises well over five hundred experiments (see below). However, with the exception of the early work of Johnston (1964) and Paul and Douglas (1965) on the simple system Na_2O-SiO_2-Fe-O, it contains only compositions with high FeO_T, for which Fe^{2+}-Fe^{3+} interactions are expected to be significant.

The results for the ~1% FeO_T composition are compared to the predictions from the equations of Kilinc et al. (1983) and Kress and Carmichael (1991) in Figure 8. Not only do these empirical equations fail to reproduce the shape of the $Fe^{3+}/\Sigma Fe$ curve (because of their non-ideal exponents), but also the positions of the curves are considerably in error.

In order to understand why this is so, it is necessary to recapitulate briefly the history of these equations. Sack et al. (1980) discussed the formulation of a thermodynamically based model to describe the Fe^{3+}/Fe^{2+} equilibrium in silicate melts. They began by writing the reaction as:

$$2Fe^{2+}O + 1/2\ O_2 = Fe_2^{3+}O_3 \tag{1a}$$
silicate melt   silicate melt

(our Reaction 1a above). They then wrote the equation for the equilibrium for this reaction (as for our Eq. 3):

$$\ln\left(\frac{X_{Fe_2^{3+}O_3}}{(X_{Fe^{2+}O})^2}\right) = \frac{-2\Delta G_r^0(1)}{RT} - \ln\left(\frac{\gamma_{Fe_2^{3+}O_3}}{(\gamma_{Fe^{2+}O})^2}\right) + \frac{1}{2}\ln f_{O_2}$$

The critical point to note about this latter equation is the use of $X_{Fe_2^{3+}O_3}$ rather than $X_{Fe^{3+}O_{1.5}}$ for the mole fraction of the Fe^{3+} species in the melt. This has two effects:

(1) The mole fraction part of the equilibrium constant for
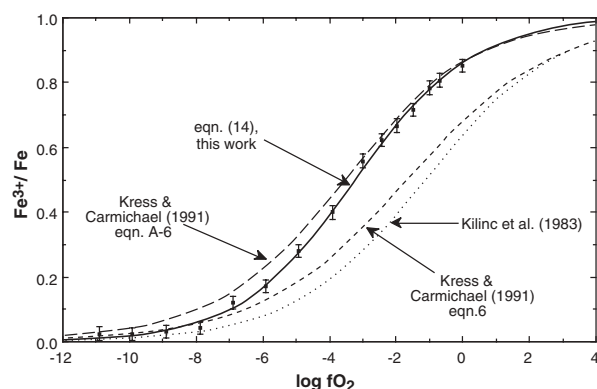
FIGURE 8. Comparison of the observed $Fe^{3+}/\Sigma Fe$ for compositions with 1 wt% FeO_T versus predictions from the empirical equations of Kilinc et al. (1983), their Equation 1, and Kress and Carmichael (1991), their Equation 6, both of which use a non-ideal exponent. The predicted curve obtained from the non-integral valence model of Kress and Carmichael (1991), their Equation A-6, which postulates mixing of FeO, $FeO_{1.5}$, and $FeO_{1.3}$ species, is a considerably better match to the data. However, Equation 14 of this work, with an ideal exponent of 0.25 and a term in $W_{Fe^{2+}-Fe^{3+}}$ to account for interactions in compositions with high FeO_T, fits the data perfectly.

the reaction is $(X_{Fe_2^{3+}O_3}/X_{Fe^{2+}O})^2$. There is no simple proportionality between this ratio and the equilibrium constant used in this work, in which the mole fraction of the Fe^{3+} species is taken as $X_{Fe^{3+}O_{1.5}}$.

(2) The ratio $[\gamma_{Fe_2^{3+}O_3}/(\gamma_{Fe^{2+}O})^2]$ does not reduce down to the simple expression of Equation 8 in the regular solution formulation. Sack et al. noted that this gave rise to an inordinate number of coefficients (they quote "approximately" 66 coefficients for a 12-component system).

Sack et al. (1980, p. 373) therefore stated that they had "chosen, at the present time, to delay the thermodynamic analysis of the ferric-ferrous data presented here in favor of developing a simpler empirical regression equation, the structure of which, though reminiscent of the thermodynamic form, should not be confused with it." Their equation was:

$$\ln\left(\frac{X_{Fe_2^{3+}O_3}}{X_{Fe^{2+}O}}\right) = a\ln f_{O_2} + \frac{b}{T} + c + \sum_i d_i X \tag{11}$$

Comparison with our Equation 10 shows that the differences, real and apparent, are:

(1) The term $\ln(X_{Fe_2^{3+}O_3}/X_{Fe^{2+}O})$ differs from $\ln(X_{Fe^{3+}O_{1.5}}/X_{Fe^{2+}O})$ simply by a constant (ln 2), hence this is not a real difference. (Note that $X_{Fe_2^{3+}O_3}$ is nearly half $X_{Fe^{3+}O_{1.5}}$).

(2) The terms d_i correspond to the $W_{Fe^{2+}-j} - W_{Fe^{3+}-j}$ terms in Equation 8, except that the latter are divided by T, implying that they are enthalpy terms. The form of Equation 11 implies entropy terms. It seems to us more likely that the interactions between species in the melt would be dominated by enthalpy terms. Empirically, though, it turns out that this makes no practical difference in how well the experimental data are fit (we tried both approaches to our own fitting of the data, and also the combination of both approaches, but the changes in the quality of the fit were only marginal). This is not, therefore, a

significant difference.

(3) The all-important term in $W_{Fe^{2+}-Fe^{3+}}$ is missing from Equation 11. We have shown that this term is required to describe the large interactions between Fe^{3+} and Fe^{2+} in the melt that our data demonstrate. What should be done if this term is not included? The answer adopted by Sack et al. (1980) was to allow the coefficient of the reaction (0.25) to vary in the regression (their a term in Eq. 11). The best fit to their data plus the previous work co-opted into their regression gave an exponent of 0.218 ± 0.007.

We now see that the probable reason for the non-ideal exponent (i.e., $a \neq 0.25$ in Eq. 11) is the omission of the term in $W_{Fe^{2+}-Fe^{3+}}$. This omission leaves no way to account for the interaction between Fe^{3+} and Fe^{2+} in the terms equivalent to non-ideal mixing of components (i.e., the d_i terms in Eq. 11); hence the slack has to be taken up by changing the exponent. This confirms what previous workers have suspected (e.g., Toplis and Corgne 2002, p. 29).

Kilinc et al. (1983) adopted the equation used by Sack et al. (1980), noting that it was "purely empirical." Kress and Carmichael (1988) subsequently pointed out that the non-stoichiometric exponent could be rationalized by invoking what they referred to as "ferric-ferrous clusters" in the melt. They found that the best fit to the experimental data was obtained when the Fe^{3+}-containing component had the stoichiometry $FeO_{1.464}$, implying the reaction: $FeO + 0.232\,O_2 = FeO_{1.464}$. Kress and Carmichael (1988) stated that the species $FeO_{1.464}$ corresponded to a complex of $FeO\cdot6Fe_2O_3$ composition, but actually it implies instead an interesting and novel concept, which is that part of the total Fe in the melt exists in a non-integral valence state, namely $Fe^{2.928+}$. Kress and Carmichael (1989), in their treatment of their data in the simple system CaO-SiO_2-Fe-O, then extended this approach by allowing for equilibrium between three species in the melt, FeO, $FeO_{1.5}$, and FeO_{1+y}, with y found empirically to be 0.3. This model therefore treats Fe in silicate melts as existing in the usual valencies of Fe^{2+} and Fe^{3+}, together with the non-integral valence state $Fe^{2.6}$. Although for practical reasons Kress and Carmichael reverted to the use of the Sack et al. (1980) empirical equation in their 1991 paper, they also discussed the application of this model to natural compositions in an Appendix (Kress and Carmichael 1991). Here we have tested their model (i.e., their equation A-6) against the results from our ~1% FeO_T composition in Figure 8. The agreement is much better than for the models with the non-ideal exponent (Kilinc et al. 1983; Kress and Carmichael 1991, their Eq. 6), although not as good as the simple model with the $W_{Fe^{2+}-Fe^{3+}}$ term used in this paper. The term in $W_{Fe^{2+}-Fe^{3+}}$ was used by Lange and Carmichael (1989) to model their results in the Na_2O-SiO_2-Fe-O system, with satisfactory results, thereby further confirming that the need for more complex models with adjustable exponents or non-integral valence states is largely due to the omission of this term.

It is standard practice in solution chemistry to investigate the stoichiometry of a dissolved species by thermodynamic methods, for example, by studying solubility as a function of ligand concentration. The same principles also apply to species in silicate melts. In much of the previous work on silicate melts, a recurring feature has been an assumption that cations with odd-numbered valencies (i.e., the cations Na^{1+}, K^{1+}, Al^{3+}, Fe^{3+}, and P^{5+}) form oxide components with two cations (i.e., Na_2O, K_2O,
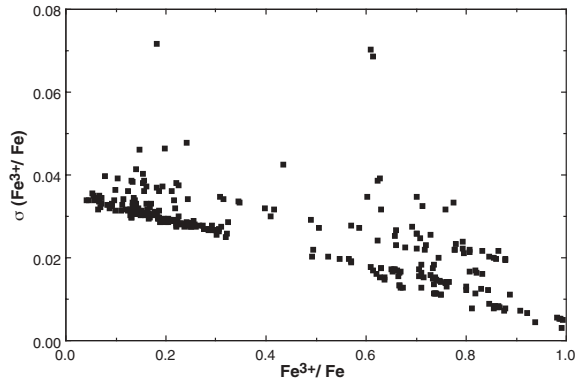
FIGURE 9. Experimental uncertainty in $Fe^{3+}/\Sigma Fe$ [$\sigma(Fe^{3+}/\Sigma Fe)$] of literature results obtained from wet-chemical analyses, assuming an uncertainty in FeO_T from electron microprobe analyses of 2% relative, and in the wet-chemical determination of FeO of $(0.02[FeO] + 0.1)$ wt%. The size of $\sigma(Fe^{3+}/\Sigma Fe)$ increases with decreasing FeO_T and decreases with $Fe^{3+}/\Sigma Fe$. By contrast, the uncertainty in $Fe^{3+}/\Sigma Fe$ from Mössbauer spectroscopy is approximately independent of both these variables.

Al_2O_3, Fe_2O_3, and P_2O_5). This implies that such cations exist as dimers in silicate melts, whereas cations with even-numbered valencies (Mg^{2+}, Fe^{2+}, Ca^{2+}, Si^{4+}) exist as monomers. This would seem unlikely and there is no independent evidence for this view. This raises the question whether or not simply using single-cation components, plus the $W_{Fe^{2+}-Fe^{3+}}$ term to take care of Fe^{2+}-Fe^{3+} interactions, can achieve a fit to the high FeO_T experimental database as good as that of the empirical equations, while also describing adequately our low FeO_T data. To address this issue, we have revisited the fitting of the data to the empirical equations of the type introduced by Sack et al. (1980). As input data, we used the following experimental results: Sack et al. (1980) = 57 data; Thornber et al. (1980) = 62 data; Kilinc et al. (1983) = 46 data; Kress and Carmichael (1988) = 46 data; Kress and Carmichael (1991) = 51 data; and Moore et al. (1995) = 31 data. This makes a total of 293 data, all at atmospheric pressure (hence anhydrous), most approximating natural aluminosilicate magmas in compositions, and, importantly, nearly all with high FeO_T (only three data have $FeO_T < 3\%$). All $Fe^{3+}/\Sigma Fe$ ratios were determined by wet-chemistry, with FeO_T being analyzed by electron microprobe. For the purposes of the regression analysis, we assumed that the experimental uncertainties (1σ) were 2% for all elements in the electron microprobe analyses, and $(0.02[FeO] + 0.1)$ wt% in the wet-chemical determination of FeO. The uncertainty in FeO was estimated from the discussions in Lange and Carmichael (1989) and Gaillard et al. (2001), plus examination of replicate analyses (e.g., in Kilinc et al. 1983, their Table 2). Experimental temperature was assigned an uncertainty of ± 2 K, and log f_{O_2} of ± 0.01 for those experiments run in air (i.e., log $f_{O_2} = 0.68 \pm 0.01$), and ± 0.05 for other conditions. Only the uncertainties in FeO_T and FeO have a significant effect. The propagation of these uncertainties gives uncertainties in $Fe^{3+}/\Sigma Fe$ that are displayed in Figure 9 for the data set. Unlike Mössbauer spectroscopy, wet-chemical analysis produces a correlation between the uncertainty in $Fe^{3+}/\Sigma Fe$ and the value of $Fe^{3+}/\Sigma Fe$ itself; also, the

uncertainty obviously becomes large as FeO_T becomes small (explaining why there are few wet-chemical data on very low FeO_T compositions).

During the course of the data fitting, we found that four samples gave conspicuously aberrant results for all models, and these four were eliminated (Ca3/123 from Thornber et al. 1980; no. 14 from Sack et al. 1980; and the duplicate experiments no. 37 and no. 38 from Kilinc et al. 1983). This leaves 289 samples in the database.

We first fitted the data to the Sack et al. (1980) model, using non-linear multiple least squares, to obtain:

$$\ln\left(\frac{X_{Fe_2^{3+}O_3}}{X_{Fe^{2+}O}}\right) = 0.1967 \ln f_{O_2} + \frac{12420}{T} - 7.054 - 0.487\, X_{MgO} + 2.201\, X_{CaO} + 6.610\, X_{Na_2O}$$
$$+ 8.214\, X_{K_2O} - 3.781\, X_{Al_2O_3} - 62.79\, X_{P_2O_5} + 1.377\, X_{FeO_t} \qquad (12)$$

where $X_{FeO_t} = X_{Fe^{2+}O} + 2X_{Fe_2^{3+}O_3}$. The value of χ_v^2 is 3.1, and the quality of the fit is illustrated in Figure 10a by plotting $Fe^{3+}/\Sigma Fe$ calculated versus observed for the 289 data. By contrast, fitting the same data using the same uncertainties to Equation 13, obtained by substituting 8 into 2,

$$\ln\left(\frac{X_{Fe^{3+}O_{1.5}}}{X_{Fe^{2+}O}}\right) = \frac{1}{4}\ln f_{O_2} - \frac{-\Delta G_r^{0}(1)}{RT} \qquad (13)$$
$$- \left(\sum_{j}^{n} X_j(W_{Fe^{3+}-j} - W_{Fe^{2+}-j})/RT + (X_{Fe^{2+}O} - X_{Fe^{3+}O_{1.5}})W_{Fe^{2+}-Fe^{3+}}/RT\right)$$

produced:

$$\ln\left(\frac{X_{Fe^{3+}O_{1.5}}}{X_{Fe^{2+}O}}\right) = \frac{1}{4}\ln f_{O_2} + \frac{16201}{T} - 8.031 - 2248\frac{X_{MgO}}{T} + 7690\frac{X_{CaO}}{T} + 8553\frac{X_{NaO_{0.5}}}{T}$$
$$+ 5644\frac{X_{KO_{0.5}}}{T} - 6278\frac{X_{AlO_{1.5}}}{T} - 63880\frac{X_{PO_{2.5}}}{T} + 6880\frac{(X_{Fe^{2+}O} - X_{Fe^{3+}O_{1.5}})}{T} \qquad (14)$$

with $\chi_v^2 = 3.8$. The fit is therefore somewhat poorer than that obtained using the empirical Sack et al. (1980) model, which seems to be largely due to a few samples at low $Fe^{3+}/\Sigma Fe$ (Fig. 10b), where the wet-chemical data are least precise (see Fig. 9). However, unlike the Sack et al. (1980) models, this equation fits the 1% FeO_T data (as it happens, perfectly, see Fig. 8).

The magnitude of the $W_{Fe^{2+}-Fe^{3+}}$ parameter ($W_{Fe^{2+}-Fe^{3+}} = -57.2$ kJ mol) is close to what we found for the AD_{eu}-FeO_T system (-47.0 ± 9.4), but the terms equivalent to $\Delta G_r^0(1)$ (i.e., $16201/T$-8.031) imply $\Delta G_r^0(1)/RT = -1.60$ at 1682 K, somewhat less negative than calculated for the AD_{eu}-FeO_T system, or expected from thermodynamic data (-2.25 ± 0.36). To reconcile these values, the melting point of Fe_2O_3 would have to be even higher than that of 2100 K assumed in deriving the thermodynamic value.

The extraordinarily high value of the coefficient for the term in $X_{PO_{2.5}}$ (or $X_{P_2O_5}$ in Eq. 12) is worthy of note. The huge effect that P_2O_5 has on stabilizing Fe^{2+} relative to Fe^{3+} in silicate melts was discovered by Mysen (1992) and confirmed by Toplis et al. (1994). The magnitude of this parameter seems unrealistic for a regular solution type of mixing model, and points toward the type of reciprocal solution model used for molten salts (Wood and Nicholls 1978).

The reason for the non-ideal exponent in the equation of Sack et al. (1980) is confirmed to arise from Fe^{2+}-Fe^{3+} interactions, as
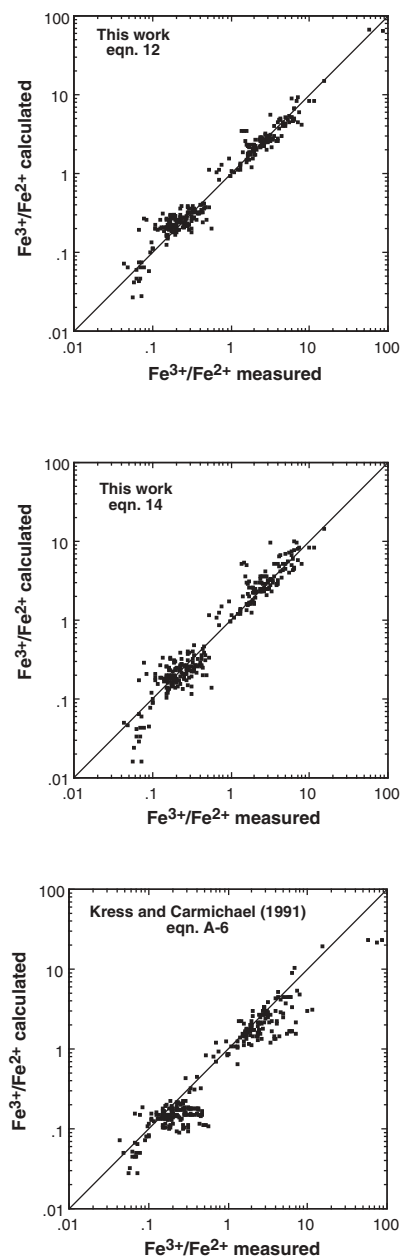
FIGURE 10. Comparison of observed with calculated $Fe^{3+}/\Sigma Fe$ for 289 data from the literature (see text), using **(a)** Equation 12 (after Sack et al. 1980); **(b)** Equation 14; and **(c)** the model of Kress and Carmichael (1991) using $Fe^{2+}O, Fe^{3+}O_{1.5}$, and the non-integral valence species $Fe^{2.6+}O_{1.3}$ (their Eq. A-6).

suggested by Kress and Carmichael (1988). However, the non-ideal exponent is an empirical fix, appearing only because there is no other term to describe these interactions in the Sack et al. (1980) equation. These interactions tend to disappear as FeO_T goes to zero, hence the ad-hoc fix does not work for low FeO_T compositions. A simple alternative model in which the regular solution formulation is carried through to its logical conclusion, and in which all cations are assumed to dissolve in the silicate melts as single-cation components (e.g., $X_{Fe^{3+}O_{1.5}}$, rather than

$X_{Fe_2^{3+}O_3}$), provides an alternative description in which the Fe^{2+}-Fe^{3+} interactions are described with the customary regular solution parameter, $W_{Fe^{2+}-Fe^{3+}}$. This equation describes the low FeO_T data well. We emphasize, however, that this equation still does not provide a truly adequate model for estimating Fe redox ratios in silicate melts. Apart from not describing the input data within their expected uncertainties (indeed, it performs less well than the Sack et al. equation in this respect), it also fails to describe adequately the experimental results from simple, alumina-free systems such as Na_2O-SiO_2-Fe-O (Lange and Carmichael 1989), and, especially, CaO-SiO_2-Fe-O (Kress and Carmichael 1989). This should not be surprising, as the regular solution model has long been known to be inadequate for silicate melts.

Following the suggestions of reviewers, we also tested some other models in the literature using the same input data, although due to the complexity of these models we have not attempted to optimize them by least-squares fitting, which we consider to be beyond the scope of the present work. The result for the model of Kress and Carmichael (1991) with the non-integral valency species (i.e., using the three species $Fe^{2+}O$, $Fe^{3+}O_{1.5}$, and $Fe^{2.6+}O_{1.3}$; their Eq. A-6) is shown in Figure 10c. There is a systematic bias to lower calculated Fe^{3+}/Fe^{2+}, meaning that optimization of this model would certainly improve the fit. To quantify the goodness of fit, we have calculated the root mean square deviation, $sqrt\{[\log(Fe^{3+}/Fe^{2+})_{calculated} - \log(Fe^{3+}/Fe^{2+})_{measured}]^2/N\}$, where $N = 289$. The value of this RMSD for this model is 0.25, which compares to RMSD values of 0.14 and 0.18 for Equations 12 and 14 of the present work, respectively. Clearly this equation performs less well than the simpler models, but it remains to be seen whether this innovative theory can provide a better fit after optimization, and with the inclusion of a full set of compositional parameters like those used in our Equations 12 and 14. The idea that the thermodynamic properties of heterovalent elements in silicate melts may require modeling using non-integral valence states could have interesting implications for such geochemically important elements as Cr, V, Nb, and U. By comparison with the models considered here, Ottonello et al. (2001) reported a RMSD of 0.20 for $N = 488$ for their model (see Ottonello et al., 2001 their Fig. 4). An assessment of earlier models has been provided by Nikolaev et al. (1996), who make the points that all models perform relatively poorly for intermediate and felsic melt compositions, and at low $Fe^{3+}/\Sigma Fe$ ratios (which is, of course, the region most relevant for most magma types). This latter factor may be due to systematic errors in wet-chemical analyses at these ratios, for which there is some circumstantial evidence (e.g., Rossano et al. 1999). The important conclusion to be emphasized here is that no model fits the data within the purported accuracy of the experimental measurements; this should provide a stimulus for further theoretical work, but also for the investigation of the accuracy of these measurements.

REFERENCES CITED

Barin, I., Sauert, F., Schultze-Rhonhof, E., and Sheng, W.S. (1989) Thermochemical data of pure substances, part I and part II, 1–1739 p. VCH Verlagsgesellschaft,

Weinheim, Germany.

Belonoshko, A. and Saxena, S.K. (1991) A molecular dynamics study of the pressure-volume-temperature properties of supercritical fluids: II. CO_2, CH_4, CO, O_2, and H_2. Geochimica et Cosmochimica Acta, 55, 3191–3208.

Berry, A.J., O'Neill, H.St.C., Jayasuriya, K.D., Campbell, S.J., and Foran, G.J. (2003) XANES calibrations for the oxidation state of iron in a silicate glass. American Mineralogist, 88, 967–977.

Borisov, A. and Jones, J.H. (1999) An evaluation of Re, as an alternative to Pt, for the 1 bar loop technique: An experimental study at 1400 °C. American Mineralogist, 84, 1528–1534.

Borisov, A.A. and Shapkin, A.I. (1990) A new empirical equation rating Fe^{3+}/Fe^{2+} in magmas to their composition, oxygen fugacity, and temperature. Geokhimiya, 6, 892–g897.

Burns, R.G. and Solberg, T.C. (1990) ^{57}Fe-bearing oxide, silicate and aluminosilicate minerals. In L.M. Coyne, S.W.S. McKeever, and D.F. Blake, Eds., Spectroscopic Characterisation of Minerals and their Surfaces, ACS Symposium Series, 415, p. 262–283. American Chemical Society, Washington, D.C.

Campbell, S.J., and Aubertin, F. (1989) Evaluation of distributed hyperfine parameters. In G.J.Long and F. Grandjean, Eds., Mössbauer Spectroscopy Applied to Inorganic Chemistry, vol. 3, p. 183–242. Plenum Press, New York.

Carmichael, I. (1991) The redox states of basic and silicic magmas—a reflection of their source regions. Contributions to Mineralogy and Petrology, 106, 129–141.

Christie, D.M., Carmichael, I.S.E., and Langmuir, C.H. (1986) Oxidation states of mid-ocean ridge basalt glasses. Earth and Planetary Science Letters, 79, 397–411.

Dyar, M.D., Naney, M.T., and Swanson, S.E. (1987) Effects of quench methods on Fe^{3+}/Fe^{2+} ratios: A Mössbauer and wet-chemical study. American Mineralogist, 72, 792–800.

Fudali, R.F. (1965) Oxygen fugacities of basaltic and andesitic magmas. Geochimica et Cosmochimica Acta, 29, 1063–1075.

Gaillard, F., Scaillet, B., Pichavant, M., and Bény, J.-M. (2001) The effect of water and f_{O_2} on the ferric-ferrous ratio of silicic melts. Chemical Geology, 174, 255–273.

Helgason, Ö., Steinthorsson S., and Mørup, S. (1992) Rates of redox reactions in basaltic melts determined by Mössbauer spectroscopy. Hyperfine Interactions, 70, 985–988.

Jing, J., Campbell, S.J., and Pellegrino, J. (1992) A stand-alone Mössbauer spectrometer based on the MC 68008 microprocessor. Measurement Science and Technology, 3, 80–84.

Johnston, W.D. (1964) Oxidation-reduction equilibria in iron-containing glass. Journal of the American Ceramic Society, 47, 198–201.

Kennedy, G.C. (1948) Equilibrium between volatiles and iron oxides in igneous rocks. American Journal of Science, 246, 529–549.

Kilinc, A., Carmichael, I.S.E., Rivers, M.L., and Sack, R.O. (1983) The ferric-ferrous ratio of natural silicate liquids equilibrated in air. Contributions to Mineralogy and Petrology, 83, 136–140.

Kress, V.C. and Carmichael, I.S.E. (1988) Stoichiometry of the iron oxidation reaction in silicate melts. American Mineralogist, 73, 1267–1274.

——— (1989) The lime-iron-silicate melt system: Redox and volume systematics. Geochimica et Cosmochimica Acta, 53, 2883–2892.

——— (1991) The compressibility of silicate liquids containing Fe_2O_3 and the effect of composition, temperature, oxygen fugacity and pressure on their redox states. Contributions to Mineralogy and Petrology, 108, 82–92.

Lange, R.A. and Carmichael, I.S.E. (1989) Ferric-ferrous equilibria in Na_2O-FeO-Fe_2O_3-SiO_2 melts: Effects of analytical techniques on derived partial molar volumes. Geochimica et Cosmochimica Acta, 53, 2195–2204.

Le Caër, G. and Dubois, J.M. (1979) Evaluation of hyperfine parameter distributions from overlapped Mössbauer spectra of amorphous alloys. Journal of Physics E, 12, 1083–90.

Moore, G., Righter, K., and Carmichael, I.S.E. (1995) The effect of dissolved water on the oxidation state of iron in natural silicate liquids. Contributions to Mineralogy and Petrology, 120, 170–179.

Murad, E. and Cashion J. (2004) Mössbauer spectroscopy of environmental materials and their industrial utilization. Kluwer Academic Publishers, Boston, pp 417.

Mysen, B.O. (1992) Iron and phosphorus in calcium silicate quenched melts.

Chemical Geology, 98, 175–202.

Mysen, B.O., Carmichael, I.S.E., and Virgo, D. (1985a) A comparison of iron redox ratios in silicate glasses determined by wet-chemical and ^{57}Fe Mössbauer resonant absorption methods. Contributions to Mineralogy and Petrology, 90, 101–106.

Mysen, B.O., Virgo, D., Neumann, E.R., and Seifert, F.A. (1985b) Redox equilibria and the structural states of ferric and ferrous iron in melts in the system CaO-MgO-Al_2O_3-SiO_2-Fe-O: relationships between redox equilibria, melt structure and liquidus phase equilibria. American Mineralogist, 70, 317–331.

Nikolaev, G.S., Borisov, A.A., and Ariskin A. A. (1996) Calculation of ferric-ferrous ratio in magmatic melts: testing and additional calibration of empirical equations for various magmatic series. Geochemistry International, 34, 641–649.

O'Neill, H.S.C. and Eggins, S.M. (2002) The effect of melt composition on trace element partitioning: an experimental investigation of the activity coefficients of FeO, NiO, CoO, MoO_2 and MoO_3 in silicate melts. Chemical Geology, 186, 151–158.

O'Neill, H.S.C. and Mavrogenes, J.A. (2002) The sulfide capacity and the sulfur content at sulfide saturation of silicate melts at 1400 °C and 1 bar. Journal of Petrology, 43, 1049–1087.

Ottonello, G., Moretti, R., Marini, L., and Vetuschi Zuccolini, M. (2001) Oxidation state of iron in silicate glasses and melts: A thermochemical model. Chemical Geology, 174, 157–179.

Paul, A. and Douglas, R.W. (1965) Ferrous-ferric equilibrium in binary alkali silicate glasses. Physics and Chemistry of Glasses, 6, 207–211.

Phillips, B. and Muan, A. (1960) Stability relations of iron oxides: Phase equilibria in the system Fe_3O_4–Fe_2O_3 at oxygen pressures up to 45 atmospheres. Journal of Physical Chemistry, 64, 1451–1453.

Popper, K. (1963) Conjectures and refutations, 431 p. Routledge, Kegan Paul, London.

Robie, R.A. and Hemingway, B.S. (1995) Thermodynamic Properties of Minerals and Related Substances at 298.15 K and 1 Bar (10^5 Pascals) Pressure and at Higher Temperatures, 461 p. United States Government Printing Office, Washington.

Rossano, S., Balan, B., Morin, G., Bauer, J.-P., Calas G., and Brouder C. (1999) ^{57}Fe Mössbauer spectroscopy of tektites. Physics and Chemistry of Minerals, 26, 530–538.

Sack, R.O., Carmichael, I.S.E., Rivers, M., and Ghiorso, M.S. (1980) Ferric-ferrous equilibria in natural silicate liquids at 1 bar. Contributions to Mineralogy and Petrology, 75, 369–376.

Thornber, C.R., Roeder, P.L., and Foster, J.R. (1980) The effect of composition on the ferric-ferrous ratio in basaltic liquids at atmospheric pressure. Geochimica et Cosmochimica Acta, 44, 525–532.

Toplis, M.J. and Corgne, A. (2002). An experimental study of element partitioning between magnetite, clinopyroxene and iron-bearing silicate liquids with particular emphasis on vanadium. Contributions to Mineralogy and Petrology, 144, 22–37.

Toplis, M.J., Dingwell, D.B., and Libourel, G. (1994) The effect of phosphorus on the iron redox ratio, viscosity, and density of an evolved ferro-basalt. Contributions to Mineralogy and Petrology, 117, 293–304.

Virgo, D. and Mysen, B.O. (1985) The structural state of iron in oxidised vs. reduced glasses at 1 atm: a ^{57}Fe Mössbauer study. Physics and Chemistry of Minerals, 12, 65–76.

Wickman, H.H., Klein, M.P., and Shirhley, P.A. (1966) Paramagnetic hyperfine structure and relaxation effects in Mössbauer spectra—Fe^{57} in ferrichrome A. Physical Review, 152, 345–357.

Wilke, M., Behrens H., Burkhard, D.J.M., Rossano, S. (2002) The oxidation state of iron in silicic melt at 500 MPa water pressure. Chemical Geology, 189, 55–67.

Wood, B.J. and Nicholls, J. (1978) The thermodynamic properties of reciprocal solid solutions. Contributions to Mineralogy and Petrology, 66, 389–400.

Wriedt, H.A. (1991) The Fe-O (iron-oxygen) system. Journal of Phase Equilibria, 12, 170–200.